arXiv:0802.2759v1 [cond-mat.str-el] 20 Feb 2008

Specific Heat Study of Magnetic and Superconducting Transitions in $CePt_3Si$

Gaku MOTOYAMA, Katsuhiro MAEDA, and Yasukage ODA

Graduate School of Material Science, University of Hyogo, Kamigori-cho, Ako-gun, Hyogo 678-1297, Japan.

Measurements of specific heat between 80 mK to 4 K and electrical resistivity between 80 mK to 10 K were carried out for polycrystalline $CePt_3Si$ samples cut into small pieces (typically ∼10 mg). In the specific heat measurements, we observed an antiferromagnetic transition jump at $T_N = 2.2$ K for all the samples, while the heights have large variations. As regards superconductivity, we observed two distinct transition jumps at $T_c^l \sim 0.45$ K and $T_c^h \sim 0.75$ K, which were the same for all the samples. From the measurements of specific heat and resistivity, systematic relations were found between antiferromagnetic and superconducting transitions. We conclude that antiferromagnetism, whose transition temperature is 2.2 K, coexists with superconductivity, whose transition temperature is T_c^l. In this sample, residual electronic specific heat coefficient in the superconducting state γ_s was quite small, and specific heat divided by temperature below T_c^l decreased almost linearly with decreasing temperature. In order to reveal the characteristic properties of the magnetism and superconductivity of the $CePt_3Si$ system, it is important to study the two superconducting phases with T_c^l and T_c^h, respectively.

KEYWORDS: $CePt_3Si$, non-centrosymmetry, antiferromagnetism, heavy fermion superconductor, specific heat measurement

1. Introduction

Bauer *et al.* reported that $CePt_3Si$ exhibits an antiferromagnetic (AFM) order at $T_N = 2.2$ K and superconducting (SC) transition at $T_c = 0.75$ K, and that normal state electronic specific heat coefficient γ_n is approx 0.39 J/(K^2·mol).[1] This compound is a heavy fermion superconductor having a characteristic crystal structure that lacks inversion symmetry (space group $P4mm$). Therefore, the superconductivity of $CePt_3Si$ exists in a particular environment compared with that of a conventional superconductor. Previous theoretical studies have shown that a non-centrosymmetric heavy fermion has several possible states for realizing unconventional superconductivity.[2–6]

Many experimental studies of superconductivity have been carried out. Previous studies of specific heat by Bauer *et al.* and Takeuchi *et al.* have shown marked contrasts between polycrystalline and single crystal samples.[1,7] The former showed a small AFM transition jump at $T_N = 2.2$ K and an SC transition jump at $T_c = 0.75$ K for a polycrystalline sample. The latter showed a large AFM transition jump at the same T_N and an SC transition jump at different T_c of 0.46 K for a single crystal sample. In the single crystal sample, the SC jump was sharp and large, and the residual electronic specific heat coefficient in the SC state, γ_s, was small, however, its T_c was low compared with that of the polycrystalline sample. In addition, a double anomaly of the SC state in the specific heat measurement was observed by Scheidt *et al.*[8] They suggest that it was a signalling two consecutive phase transitions. On the other hand, Nakatsuji *et al.* showed that the Meissner effect of SC started increasing from ∼ 0.8 K and the rate of increase changed below ∼ 0.5 K.[9] They suggest that the SC domain has a volume fraction. The pressure dependence of the Meissner effect and T_c seemed to indicate that the volume fraction was due to some inhomogeneous property that leads to a spatial variation of local pressure in the sample.[10]

The temperature T dependence of specific heat divided by temperature (C/T) in the SC region preferred a linear T dependence over a $T^{-1}\exp(-\Delta/k_BT)$ dependence.[7] In addition, the T dependence of thermal conductivity in the T range of 40 mK to 0.2 K was well fitted by a linear function of T.[11] These results indicate the presence of line nodes in the SC energy gap. On the other hand, the T dependence of nuclear spin-lattice relaxation rate $1/T_1(T)$ did not simply follow an exponential law or a T^3-power law. The plot of $1/T_1T(T)$ showed a coherence Hebel-Slichter peak at T_c, indicating a full-gap state without nodes.[12] Another NMR measurement indicated that the plot of $1/T_1(T)$ showed no obvious Hebel-Slichter peak and a drastically decreasing ($\propto T^3 \sim T^5$).[13,14] Therefore, $CePt_3Si$ is expected to be an unconventional superconductor. In addition, the pressure P phase diagram of T_c and T_N for this system was unusual compared with that of the previous magnetic superconductor.[15–17] Although T_c and T_N decreased with increasing P, SC still existed even after AFM disappeared. The decreasing rate of T_c slowed down only at around P_c, at which AFM disappeared. The pressure corresponding to the maximum T_c in this system was not P_c. Some heavy fermion magnetic superconductors show a dome structure for the pressure dependence of T_c at the critical point P_c.

2. Experimental

Polycrystalline $CePt_3Si$ and $Ce_{1.01}Pt_3Si$ samples were synthesized by arc-melting Ce of 99.9 % (3N) purity, Pt of 3N5 purity, and Si of 6N purity, using a laboratory-made furnace. The synthesized melt became solidified by quenching on Cu-hearth in Ar atmosphere of 6N purity. The chemical compositions of our samples were deter-

mined from those of the starting materials. The weight loss of the constituent materials was negligible during the preparation. An ingot sample (1∼2 g) was cut into two lumps, and one lump was heat-treated. Heat treatment for annealing was carried out under well-controlled conditions: the temperature was maintained at 950°C for one week and lowered to room temperature over three days. We labeled heat-treated and non-heat-treated samples as "annealed" and "as-cast", respectively. Then, each lump was cut into small pieces (∼ 10 mg) for measurement. We prepared three $CePt_3Si$ as-cast (#1, 2 and 3), two $Ce_{1.01}Pt_3Si$ as-cast (#4 and 5), and their annealed samples (#1-a, #2-a and so on) to investigate sample dependence.[18,19] Moreover, we conducted measurements using different pieces from the same batch (#2-a-1, #2-a-2, and so on).

Temperature dependence of specific heat was measured using the adiabatic heat pulse method between ∼80 mK to 4 K. Electrical resistivity was measured using the conventional dc four-terminal method down to ∼80 mK using the same piece as that used in specific heat measurement. Measurements were carried out using a laboratory-made dilution refrigerator.

3. Results and Discussion

Figure 1(a) shows the T dependence of specific heat divided by T (C/T) of the $CePt_3Si$ as-cast (#1) and $Ce_{1.01}Pt_3Si$ annealed (#4-a-2) samples. They showed quite different characteristics despite having the same polycrystalline $CePt_3Si$ system. The $C/T(T)$ of the $Ce_{1.01}Pt_3Si$ annealed showed a distinct AFM transition with a large jump at T_N (= 2.2 K) and SC transition with a sharp jump at low T_c (= 0.45 K). The residual γ_s extrapolated to 0 K was almost zero. These results were similar to those reported by Takeuchi *et al.* for their single crystal, as shown by the solid line. On the other hand, the $C/T(T)$ of $CePt_3Si$ as-cast exhibited a very small jump of AFM transition and a jump of SC transition appearing at high T_c (=0.75 K) compared with that of $Ce_{1.01}Pt_3Si$ annealed. The AFM transition of this sample had not only a small jump but also a broad tail above T_N, from 2.2 K to ∼ 4.0 K. $C/T(T)$ clearly increased at the onset of T_c with decreasing T, but the peak broadened. These behaviors were similar to that observed by Bauer *et al.* for their polycrystalline sample, as shown by the broken line. Figure 1(b) shows the temperature dependence of the electrical resistivity (ρ) of the $CePt_3Si$ as-cast and $Ce_{1.01}Pt_3Si$ annealed samples. Measurements were carried out using very small pieces. Because the absolute value might include some ambiguity, $\rho/\rho_{4K}(T)$ values are presented. The residual resistivity ratio (RRR) of $CePt_3Si$ as-cast was 20 and that of $Ce_{1.01}Pt_3Si$ annealed was 120. We confirmed reproducibility by some measurements. All of the measured $Ce_{1.01}Pt_3Si$ annealed including different batches had RRR exceeding 100. These were remarkably large, but other measured samples indicated RRR ∼ 20. A kink of $\rho/\rho_{4K}(T)$ was observed at T_N=2.2 K for both samples. The $\rho/\rho_{4K}(T)$ of the $Ce_{1.01}Pt_3Si$ annealed showed a clear kink at T_N and decreased rapidly below T_N with decreasing temperature. The decrease plateaued

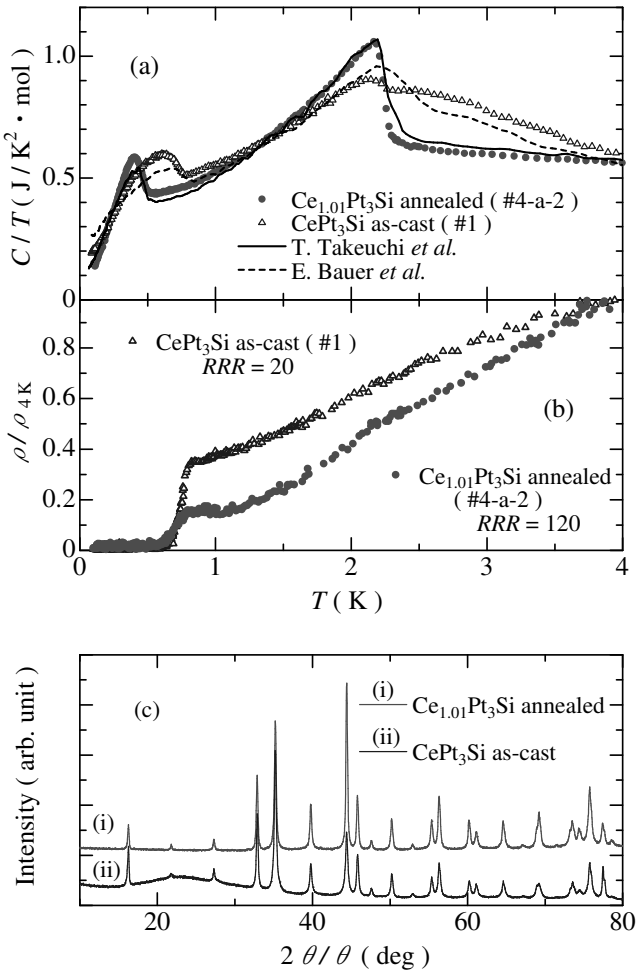

Fig. 1. (a) Temperature dependence of specific heat divided by temperature, C/T, for $CePt_3Si$ as-cast (#1) and $Ce_{1.01}Pt_3Si$ annealed (#4-a-2). The solid line shows data obtained by Takeuchi *et al.* (ref. 7), and the broken line shows data of Bauer *et al.* (ref. 1). (b) Temperature dependence of electrical resistivity, which was measured using the same pieces as those in Fig. 1(a). $CePt_3Si$ as-cast (#1) had a small residual resistivity ratio (RRR) of 20; $Ce_{1.01}Pt_3Si$ annealed (#4-a-2) had a large RRR of 120. (c) X-ray diffraction patterns of samples from the same batch as those shown in Figs. 1(a) and 1(b). Pattern (ii) contained a larger background effect than pattern (i).

immediately just above T_c. On the other hand, the kink of the $\rho/\rho_{4K}(T)$ of the $CePt_3Si$ as-cast broadened, and the decrease of $\rho/\rho_{4K}(T)$ continued to T_c. These results of $C/T(T)$ and $\rho/\rho_{4K}(T)$ indicate that $Ce_{1.01}Pt_3Si$ annealed has a more regular AFM ordering (which is a long-range ordering with a narrow T_N at 2.2 K) and a more regular lattice (which is an ideal $CePt_3Si$ lattice, that is a non-centrosymmetric lattice) than $CePt_3Si$ as-cast. Figure 1(c) shows the X-ray diffraction patterns. No extra-phase was observed in the X-ray diffraction patterns of both samples. There was no difference in the accuracy of measurement between the lattice constants of the two samples. The results in Fig. 1 indicate that 1% variations in Ce-concentration and heat treatment yield small structural changes that strongly affect SC and AFM but not powder diffraction patterns. In our speculation, these structural changes concern the

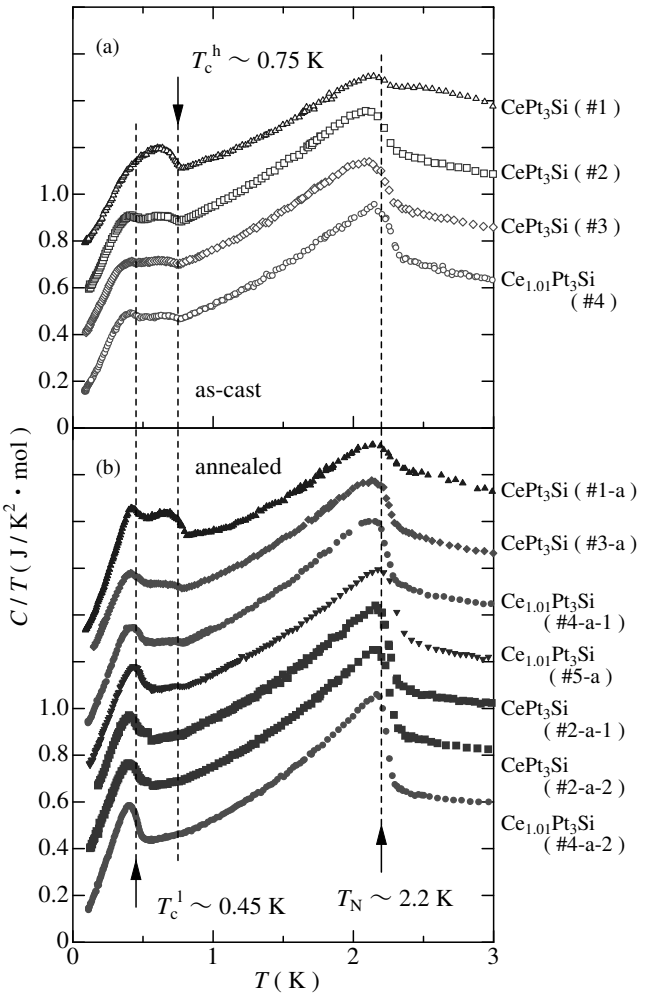

Fig. 2. T dependences of C/T for $CePt_3Si$ and $Ce_{1.01}Pt_3Si$. Experimental data were shifted upward by 0.2 J/(K^2·mol) intervals. Data with open (closed) symbols in Figs. 2(a) and 2(b) were respectively measured using as-cast and annealed samples. T_N is the antiferromagnetic ordering temperature, and bulk superconductivity occurs below T_c^l and/or T_c^h. Each sample was denoted as #(sample number)-('a': annealed)-(piece number).

non-centrosymmetric structure, which is an ordering of Pt and Si atoms occupying the two 1(a)-sites of the $P4mm$ structure. Because, it is considered that non-centrosymmetricity is important for both SC of this system and AFM whose magnetic structure consists of ferromagnetic c-planes stacked antiferromagnetically along the c-axis.[20] Therefore, although $Ce_{1.01}Pt_3Si$ annealed has 1% opening Pt and Si sites, it might have two well-ordered 1(a)-sites of $P4mm$ occupied by Pt and Si atoms. Then, the opening sites might be available for removing and ordering Pt and Si atoms when a sample is heat-treated. Conversely, although $CePt_3Si$ as-cast has a stoichiometric composition, it might have some disorders of Pt and Si at the two 1(a)-sites, because there is a quenching process in the preparation of polycrystalline samples.

Figures 2(a) and 2(b) show the $C/T(T)$ of various samples in order to consider sample dependence in detail. Fig. 2(a) shows the results for the as-cast samples and Fig. 2(b) shows those for the annealed samples. In Figs. 2(a) and 2(b), the data were arranged according to the decrease in the height of the specific heat jump in AFM transition from bottom to top. First, we note both AFM and SC transitions, respectively. The height of the jump in AFM transition, $\Delta C/T(T_N)$, decreased gradually without changing T_N, and the broad tail above T_N enlarged gradually from the bottom to top data. This relation is plotted in Fig. 3(b). We observed two peaks for SC transition in both Figs. 2(a) and 2(b). We define T_c^l (~ 0.45 K) as the temperature of the specific heat peak at lower and T_c^h (~ 0.75 K) as the onset temperature of the specific heat peak at higher. T_c^l and T_c^h were almost constant for all the samples. However, the heights of the specific heat jump at T_c^l and T_c^h, $\Delta C/T(T_c^l)$ and $\Delta C/T(T_c^h)$, differed for each sample. As $\Delta C/T(T_c^l)$ increased, $\Delta C/T(T_c^h)$ decreased. These results indicate that T_c^l does not move to T_c^h and that the SC at T_c^l and T_c^h compete against each other. $CePt_3Si$ as-cast (#1) has only one large peak at T_c^h. However, this peak might include some components of $\Delta C/T(T_c^l)$, because it is broadened from T_c^h to T_c^l. Unfortunately, we were unable to prepare a sample that shows only a sharp jump at T_c^h and a small residual γ_s. Next, the relations between the two SC transition jumps, $\Delta C/T(T_c^l)$ and $\Delta C/T(T_c^h)$, and the AFM transition jump, $\Delta C/T(T_N)$, should be noted. In Figs. 2(a) and 2(b), $\Delta C/T(T_c^l)$ increased from the top to bottom data, that is, as $\Delta C/T(T_N)$ increased, $\Delta C/T(T_c^l)$ increased as well. The most typical example of this case is $Ce_{1.01}Pt_3Si$ annealed (#4-a-2). $\Delta C/T(T_c^h)$ increased from the bottom to top data. It should be noted that $\Delta C/T(T_N)$ and $\Delta C/T(T_c^l)$ almost vanished in the sample with the largest $\Delta C/T(T_c^h)$. These data of correlation between $\Delta C/T(T_c^h)$, $\Delta C/T(T_c^l)$ and $\Delta C/T(T_N)$ are plotted in Fig. 3(a). These relations are described later. Next, we compare the annealed samples in Fig. 2(b) with the as-cast samples in Fig. 2(a). The $\Delta C/T(T_N)$ and $\Delta C/T(T_c^l)$ of the annealed samples were almost larger than those of the as-cast samples, while the γ_s of the annealed samples were smaller than those of the as-cast samples. These results are shown in Figs. 3(a) - 3(c) as open and closed symbols for as-cast and annealed, respectively.

The relations of $\Delta C/T(T_c^h)$, $\Delta C/T(T_c^l)$, $C/T(2.4\text{ K})$ and γ_s versus $\Delta C/T(T_N)$ are plotted in Figs. 3(a) - 3(c), respectively. In Fig. 3(a), when $\Delta C/T(T_N)$ increases, $\Delta C/T(T_c^h)$ decreases and $\Delta C/T(T_c^l)$ increases. It is clear that SC at T_c^h and T_c^l compete against each other, and that SC at T_c^h is on competitive relation with AFM at T_N but SC at T_c^l is not. In Fig. 3(b), $C/T(2.4\text{ K})$, which reflects the broad tail above T_N, increased with decreasing $\Delta C/T(T_N)$. This enhancement might have some relation with an increase in $\Delta C/T(T_c^h)$. In Fig. 3(c), the relation between γ_s and $\Delta C/T(T_N)$ is not clear, but at least the γ_s of as-cast was large and the γ_s of annealed with a large $\Delta C/T(T_N)$ was small. $\Delta C/T(T_c^l)$, $\Delta C/T(T_c^h)$ and $\Delta C/T(T_N)$ were decided in accordance with Fig. 3(d). These absolute values have some ambiguities because of their broadness. However, it has no significant effects on their relations.

As mentioned above, the present experiment leads us to conclude that the $CePt_3Si$ system is spatially separated into two superconducting regions, SC^l and SC^h,

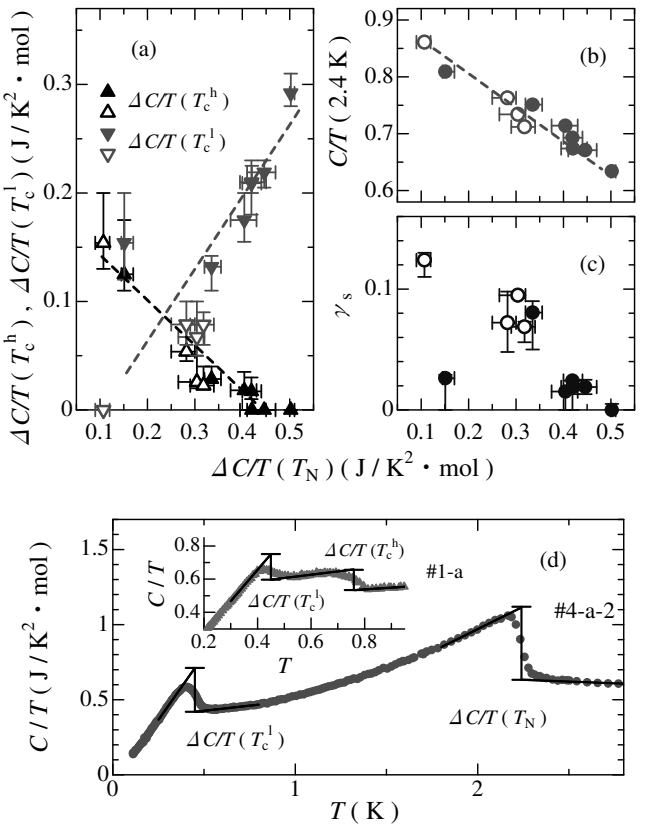

Fig. 3. Relations of $\Delta C/T(T_c^l)$, $\Delta C/T(T_c^h)$, C/T(2.4 K) and γ_s versus $\Delta C/T(T_N)$ are plotted in Fig. 3(a) - 3(c), respectively. The broken lines are guides to the eye. Open and closed symbols indicate the results of as-cast and annealed, respectively. $\Delta C/T(T_c^l)$ ($\Delta C/T(T_c^h)$, $\Delta C/T(T_N)$) was determined by a linear extrapolation of the $C/T(T)$ data below T_c^l (T_c^h, T_N) and above T_c^l (T_c^h, T_N) to T_c^l (T_c^h, T_N), as indicated in Fig. 3(d). γ_s was decided by linear extrapolation to 0 K.

whose transition temperatures are T_c^l ($\sim$ 0.45 K) and T_c^h ($\sim$ 0.75 K), respectively. SC^l develops in a more regular AFM ordering and a more regular lattice. $Ce_{1.01}Pt_3Si$ annealed (#4-a-2) is considered to have an almost single phase in which SC^l and AFM with T_N coexist. Because, the volume fraction of this sample exhibited SC^l with a particularly small residual γ_s and AFM with the most distinct and largest peak for this sample are probably bulk properties. On the other hand, SC^h does not seem to coexist with AFM having T_N=2.2 K at least. In what kind of phase is this SC^h included? To answer this question, the broad tail gradually enlarging above T_N might give us some hints. We suggest that the region of SC^h is included in some magnetic phase which causes enhancement of the broad tail above T_N (for example, a heavy fermion non magnetic phase and an AFM phase with broad T_N from 2.2 to 4.0 K.[21]) We suggested in our earlier discussion of Fig. 1 and in refs. 18 and 19 that as-cast samples contain some defects, which are reduced in number by heat treatment and annealing. The annealed samples exhibit large *RRR*, a marked transition at a narrow T_N and a less ferromagnetically anomaly at 3.0 K. A sample having a perfectly regular structure would have perfect non-centrosymmetry. The presence of some defects will affect non-centrosymmetry and produce some partial disorders. In particular, we consider Pt and Si atoms occupying the two 1(a)-sites of the $P4mm$ structure as important parts. From this viewpoint, there is a relation between the inhomogeneity of this system and the two volume fractions of SC^l and SC^h. The as-cast sample that has some disorders in the non-centrosymmetric structure exhibits a large volume fraction of SC^h, and the annealed sample with well-ordered non-centrosymmetricity exhibits a large volume fraction of SC^l. It might be implied that SC^h develops in the centrosymmetric part and SC^l develops in the non-centrosymmetric part.

Here, we need to explain why the regular lattice has a low superconducting transition temperature, T_c^l. From the above sample characterization, we found that SC was affected by the AFM state and the disorder of the non-centrosymmetric structure. We suggest three scenarios to explain T_c^l. (i) One scenario is that SC^h exists in the non magnetic heavy fermion state in contrast to the coexistence of SC^l and AFM at T_N of 2.2 K. T_c^l might be reduced by an internal magnetic field of AFM. In this case, the broad tail of $C/T(T)$ above T_N is due to a non magnetic heavy fermion state. (ii) The second scenario is that SC^h exists in another inhomogeneous AFM phase with a broad transition temperature from 2.2 K to 4.0 K, T_N^h. This inhomogeneous AFM phase transition is the cause of the broad tail. This scenario is consistent with the P-T phase diagram. In the P-T phase diagram, T_c and T_N decrease with increasing pressure. If effective pressure caused by the inhomogeneity of a lattice were reduced in the region of SC^h, the enhancement to T_c^h and the broad tail of T_N^h could be explained.[10] A degree of the inhomogeneity causes a broad T_c^h and a broad tail of T_N^h. (iii) The third scenario is that SC^l exists in a well-ordered non-centrosymmetric region and SC^h exists in a disordered region. Some previous theoretical works have shown that T_c is suppressed by enhancing antisymmetric spin-orbit coupling.[5,6] In general, antisymmetric spin-orbit coupling is weakened by the disorder of a non-centrosymmetric structure. Therefore, T_c^l was suppressed by enhancing antisymmetric spin-orbit coupling, and T_c^h was hardly suppressed. These are simple illustrations. In fact, it might be described by combining the above scenarios and others.

Figure 4 shows the magnified $C/T(T)$ of the $Ce_{1.01}Pt_3Si$ annealed (#4-a-2) and $CePt_3Si$ as-cast (#1) samples below 1 K. The former exhibited the largest jump at T_c^l, while the latter exhibited the largest jump at T_c^h. As shown in the figure, the C/T of sample #4-a-2 decreased linearly to temperatures below T_c^l and the extrapolated residual γ_s to 0 K was very small. In contrast, the C/T of sample #1 seemed to have a different temperature dependence, and the extrapolated residual γ_s to 0 K was finite. In order to reveal the T dependence of C/T below T_c^h, we need to prepare a sample with only a sharp jump at T_c^h and a small residual γ_s.

4. Conclusions

In conclusion, we observed an AFM transition jump in specific heat measurements of the polycrystalline $CePt_3Si$ system. We observed T_N = 2.2 K for all the measured pieces, but $\Delta C/T(T_N)$ tended to vary among

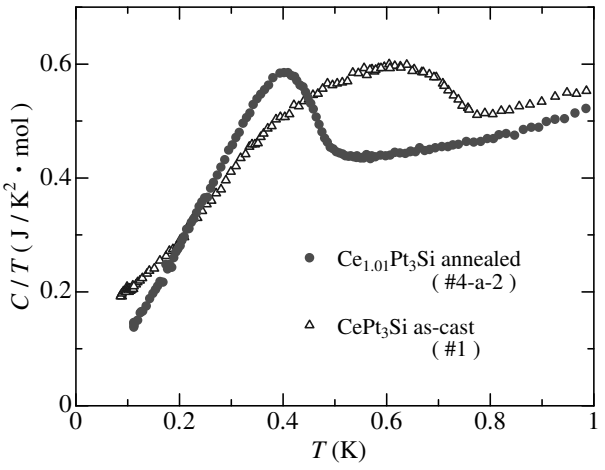

Fig. 4. T dependences of C/T below 1 K for $Ce_{1.01}Pt_3Si$ annealed and $CePt_3Si$ as-cast.

pieces. As $\Delta C/T(T_N)$ decreased, a broad tail above T_N enlarged gradually. We observed two SC transition jumps at T_c^l and T_c^h, which showed no sample dependence. SC^l and SC^h volume fractions are considered to be spatially separated to each other in a piece. A larger $\Delta C/T(T_c^l)$ appeared in a piece that showed a larger $\Delta C/T(T_N)$. In contrast, a larger $\Delta C/T(T_c^h)$ appeared in a piece that showed a smaller $\Delta C/T(T_N)$. Moreover, the piece with the largest jump at T_c^l had a small γ_s and the largest RRR, and these properties appeared in both heat-treated and annealed pieces. Thus, SC^l was concluded to coexist with the AFM having $T_N = 2.2$ K in a regular lattice as non-centrosymmetricity. The volume fractions of SC^l and SC^h change with the state of AFM ordering and the defects in crystal structures.

Acknowledgments

We thank A. Sumiyama, T. Kohara, K. Ueda, and Y. Hasegawa for helpful discussions. This work was partially supported by a Grant-in-Aid for Scientific Research from the Ministry of Education, Culture, Sports, Science and Technology, Japan.

1) E. Bauer, G. Hilscher, H. Michor, Ch. Paul, E. W. Scheidt, A. Gribanov, Yu. Seropegin, H. Noël, M. Sigrist, and P. Rogl: Phys. Rev. Lett. **92** (2004) 027003.
2) P. A. Frigeri, D. F. Agterberg, A. Koga, and M. Sigrist: Phys. Rev. Lett. **92** (2004) 097001.
3) S. Fujimoto: J. Phys. Soc. Jpn. **75** (2006) 083704.
4) N. Hayashi, K. Wakabayashi, P. A. Frigeri, and M. Sigrist: Phys. Rev. B. **73** (2006) 024504.
5) H. Tanaka, H. Kaneyasu, and Y. Hasegawa: J. Phys. Soc. Jpn. **76** (2007) 024715.
6) Y. Yanase and M. Sigrist: J. Phys. Soc. Jpn. **76** (2007) 043712.
7) T. Takeuchi, T. Yasuda, M. Tsujino, H. Shishido, R. Settai H. Harima, and Y. Ōnuki: J. Phys. Soc. Jpn. **76** (2007) 014702.
8) E-W. Scheidt, F. Mayr, G. Eickerling, P. Rogl and E. Bauer: J. Phys.: Condens. Matter **17** (2005) L121.
9) K. Nakatsuji, A. Sumiyama, Y. Oda, T. Yasuda, R. Settai and Y. Ōnuki: J. Phys. Soc. Jpn. **75** (2006) 084717.
10) Y. Aoki, A. Sumiyama, G. Motoyama, Y. Oda, T. Yasuda, R. Settai and Y. Ōnuki: J. Phys. Soc. Jpn. **76** (2007) 114708.
11) K. Izawa, Y. Kasahara, Y. Matsuda, K. Behnia, T. Yasuda, R. Settai, and Y. Ōnuki: Phys. Rev. Lett. **94** (2005) 197002.
12) M. Yogi, Y. Kitaoka, S. Hashimoto, T. Yasuda, R. Settai, T. D. Matsuda, Y. Haga, Y. Ōnuki, P. Rogl, and E. Bauer: Phys. Rev. Lett. **93** (2004) 027003.
13) K. Ueda, K. Hamamoto, T. Kohara, G. Motoyama and Y. Oda: Physica B. **359-361** (2005) 374.
14) K. Ueda, T. Kohara, G. Motoyama and Y. Oda: J. Mag. Mag. Mat. **310** (2007) 608.
15) T. Yasuda, H. Shishido, T. Ueda, S. Hashimoto, R. Settai, T. Takeuchi, T. D. Matsuda, Y. Haga and Y. Ōnuki: J. Phys. Soc. Jpn. **73** (2004) 1657.
16) N. Tateiwa, Y. Haga, T. D. Matsuda, S. Ikeda, T. Yasuda, T. Takeuchi, R. Settai and Y. Ōnuki: J. Phys. Soc. Jpn. **74** (2005) 1903.
17) E. Bauer, H. Kaldarar, A. Prokofiev, E. Royanian, A. Amato, J. Sereni, W. Brämer-Escamilla, and I. Bonalde: J. Phys. Soc. Jpn. **76** (2007) 051009.
18) G. Motoyama, S. Yamamoto, H. Takezoe, Y. Oda, K. Ueda and T. Kohara: J. Phys. Soc. Jpn. **75** (2006) 013706.
19) G. Motoyama, M. Watanabe, K. Maeda, Y. Oda, K. Ueda and T. Kohara: J. Mag. Mag. Mat. **310** (2007) e126.
20) N. Metoki, K. Kaneko, T. D. Matsuda, A. Galatanu, T. Takeuchi, S. Hashimoto, T. Ueda, R. Settai, Y. Ōnuki and N. Bernhoeft: J. Phys.: Condens. Matter **16** (2004) L207.
21) W. Higemoto, Y. Haga, T. D. Matsuda, Y. Ōnuki, K. Ohishi, T. U. Ito, A. Koda, S. R. Saha and R. Kadono: J. Phys. Soc. Jpn. **75** (2006) 124713.